Quantum Electronics **49** (9) 824–831 (2019)

INTERACTION OF LASER RADIATION WITH MATTER. LASER PLASMA https://doi.org/10.1070/QEL16869

Laser formation of luminescence bubble microstructures in polymer films

A.O. Rybaltovskiy, A.A. Akovantseva, V.F. Burdukovskiy, L.I. Krotova, N.V. Minaev, P.S. Timashev, B.Ch. Holhoev, V.I. Yusupov

Abstract. **The results of laser-induced formation of luminescent structures on the surface of poly-2.2′-*n*-oxydiphenylene-5.5′-bis-benzimidazole films, obtained by the coating method from a formic acid solution, are presented. The structures are formed using cw 405-nm laser radiation with intensities of 10^2–10^4 W cm^{-2}. It is shown (using methods of optical, atomic-force, and electron microscopy) that the structures formed on the surface are microbubble foam-like aggregations. Their formation is modelled as a sequence of the following processes: release of formic acid molecules, their condensation on matrix defects in the surface layer, and explosive boiling as a result of heating this layer of polymer film by the laser beam. The luminescence of these structures is due to the weakening of the concentration quenching from closely spaced luminescence centres in benzimidazole cycles during their emergence to the surface and the increase in the distance between them due to the extension on bubble aggregates on the surface.**

Keywords: *polybenzimidazole, laser radiation, bubble structures, luminescence, concentration quenching.*

1. Introduction

The laser-induced formation of surface microstructures is often related to a local change in the refractive index or absorption and scattering coefficients. For example, structures with a gradient material density of micron and submicron sizes can be formed in pure glasses under irradiation by femtosecond laser pulses (see, e.g., [1–4]). Due to the formation of metal nanoparticles exhibiting plasmonic absorption [5], irradiation of glasses impregnated with silver precursors by laser pulses may lead to the formation of microstructures characterised by high absorption and scattering coefficients. As was experimentally shown in [6, 7], similar structures can also be obtained in polymer matrices containing metal precursors under cw laser irradiation. Interest in the formation of various microstructures, including Bragg gratings, is due to the intense development of the element base for photonics and sensorics [8, 9]. A number of studies in this field were aimed at forming laser-induced extended luminescence structures in various transparent materials. For example, the possibility of designing miniature luminescence waveguides using femtosecond radiation was demonstrated in [8, 9] by the example of a derivative of MEH-PPV polymer (poly-[2-methoxy-5-(2′-ethylhexyl-oxy)-*p*-phenylene-vinylene]), which luminesces initially in the red region. Adding Rhodamine 610 to this polymer matrix in the same way makes it possible to form other luminescent micrometer-sized structures [10], which can be used in optoelectronics as sensing elements.

In our opinion, especially interesting is another approach, in which luminescent centres, combined into structures in the bulk or in the surface layer, are formed in the initial matrix due to the laser effect, without applying any special additives. It was shown in [11, 12] that fairly stable luminescent radicals are formed in polymer (polymethylmethacrylate, polystyrene) matrices under femtosecond laser irradiation. The possibility of forming luminescent foam-like structures in a gelatin matrix by pulsed laser radiation was demonstrated in [13–15]. Previously, we were the first to observe the formation of luminescent bubble structures in the bulk of heat-resistant polymer poly-2.2′-*n*-oxydiphenylene-5.5′-bis-benzimidazole (OPBI) irradiated by a cw 405-nm laser [16]. Foam-like luminescent structures were also observed along the entire boundary of the laser channels formed in a water-saturated polymer matrix when moving a laser beam along its surface [17].

The purpose of this study was to analyse in detail the possibility of forming luminescent structures on the surface of OPBI-based film samples irradiated by a cw 405-nm laser. It is of interest to study the mechanism of the formation of these structures, because one can determine in this way the specific features of the physicochemical processes of laser-induced transformation in a matrix of heterochain polymers with a high content of another component (formic acid, used as a solvent). Of great practical interest is the possibility of precise formation of various porous microstructures on the surface of polymer films. Due to the high specific surface area, these structure can be used for efficient impregnation and adsorption of various materials in order to impart new functional properties (e.g., luminescent and plasmonic) to them.

A.O. Rybaltovskiy D.V. Skobeltsyn Institute of Nuclear Physics, M.V. Lomonosov Moscow State University, Vorob'evy gory, 119991 Moscow, Russia; Institute of Photonic Technologies, Federal Scientific Research Centre 'Crystallography and Photonics', Russian Academy of Sciences, ul. Pionerskaya 2, Troitsk, 108840 Moscow, Russia;
A.A. Akovantseva, L.I. Krotova, N.V. Minaev, V.I. Yusupov Institute of Photonic Technologies, Federal Scientific Research Centre 'Crystallography and Photonics', Russian Academy of Sciences, ul. Pionerskaya 2, Troitsk, 108840 Moscow, Russia; e-mail: minaevn@gmail.com;
V.F. Burdukovskiy, B.Ch. Holhoev Baikal Institute of Nature Management, Siberian Branch, Russian Academy of Sciences, ul. Sakh'yanovoi 6, 670047 Ulan-Ude, Russia;
P.S. Timashev Institute of Photonic Technologies, Federal Scientific Research Centre 'Crystallography and Photonics', Russian Academy of Sciences, ul. Pionerskaya 2, Troitsk, 108840 Moscow, Russia; Institute for Regenerative Medicine, I.M. Sechenov First Moscow State Medical University, ul. Trubetskaya 8, stroenie 2, 119991 Moscow, Russia; Semenov Institute of Chemical Physics, Russian Academy of Sciences, ul. Kosygina 4, Moscow, 119991 Russia

Received 24 October 2018; revision received 14 April 2019
Kvantovaya Elektronika **49** (9) 824–831 (2019)
Translated by Yu.P. Sin'kov

2. Experimental

To form luminescent structures in a polymer matrix, we used samples of heat-resistant OPBI films, obtained by the coating method from a solution of formic acid (HCOOH) and dried in air for two weeks at a temperature of 23 °C The thickness of the experimental films varied in the range of 40–80 μm. The residual content of acid molecules in the dried films did not exceed 10 wt %. The synthesis conditions were described in detail in [16], where the presence of luminescence from the film surface areas exposed to a focused cw 405-nm laser beam was reported for the first time. It was found in [18] that initial OPBI solutions in formic acid exhibit pronounced luminescence with characteristic peaks in the vicinity of 398 and 410 nm, whose intensity decreases with an increase in the OPBI concentration in the solution.

The photoinduced formation of extended structures on the surface of OPBI films was performed on a setup whose schematic is shown in Fig. 1. A solid-state laser module (405 nm) with diode pumping (MDL-III-405, People's Republic of China) was used; the cw laser power was varied from 30 to 90 mW in the experiments. The laser beam was focused (using a planar microscopic 10× objective (NA = 0.3, F = 6 mm) on the surface of a three-axis motorised translation stage, with a film sample horizontally mounted on it. The structures were formed by displacing the stage with a sample with respect to the laser beam focus. The laser beam intensity on the film surface reached 10^4 W cm^{-2} in the experiments. The spot diameter was set by changing the distance from the sample to the objective; the irradiation was monitored using a digital video camera (ToupTek XFCAM1080PHB, People's Republic of China) with a telescopic objective and an autofocusing module, which made it possible to obtain surface images of irradiated samples. Under conditions of exact laser beam focusing on the sample surface, the spot diameter amounted to 10–20 μm (at the level of 1/e^2).

Using this system to form linear structures, one can investigate their formation dynamics during irradiation in different regimes. Structures shaped as separate lines were obtained in experiments at different laser beam intensities on the film surface (to this end, the sample was shifted relative to the objective focal plane) and at different laser beam scanning velocities over the sample surface.

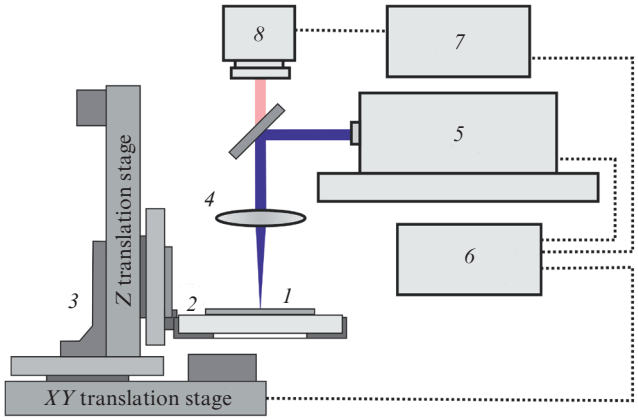

Figure 1. Schematic of the facility for laser-induced formation of structures in film samples:
(*1*) polymer film; (*2*) quartz plate in a mounting; (*3*) *XYZ* motorised translation stage; (*4*) microlens; (*5*) laser (λ = 405 nm); (*6*) controller; (*7*) control computer; (*8*) digital video camera.

The thus formed structures were investigated by the methods of luminescence and optical 3D microscopy, atomic force microscopy (AFM), and scanning electron microscopy (SEM).

Using optical 3D microscopy, one can obtain general information about the morphology of laser-induced structures in polymer films under different formation conditions. In this method, a series of images are recorded with displacement along the vertical axis (the displacement step is ~1–2 μm), and then they are subjected to computer processing to obtain topographic images of the sample relief. Images were recorded using a 3D microscope HRM-300 Series (Huvitz, Korea) with objectives 5× and 10× and a digital camera HM-TV0.5XC (Huvitz, Korea).

The luminescence intensity from the sample surface was recorded with a MC300 microscope (Micros, Austria), equipped with a luminescence block, a digital camera DCM510, and a long-focal-length objective 10×/0.25 LMPlanFLN (Olympus, Japan). Luminescence was excited using the blue (435 nm) and green (546 nm) bands of the luminescence unit with a mercury lamp. When studying the temperature effects related to the film luminescence, a sample was mounted on a disk heater (located under the microscope objective), which provides programmable heating up to 80 °C.

Individual bubble aggregates on the film surface were investigated by AFM, which made it possible to analyse their micro- and nanorelief. Measurements were performed on a Multi Mode 8 microscope (Bruker, United States) with a maximum scan area of 14 × 14 μm. The effect of cw laser radiation on the OPBI film surface was also studied using a scanning electron microscope LEO 1450 (Karl Zeiss, Germany). Film samples were placed on a standard conducting carbon adhesive tape; a (15–20)-nm-thick gold–palladium layer was formed on the tape surface by cold plasma deposition to provide a desired electrical conductivity. The films were studied at an accelerating voltage of 10 kV.

The luminescence spectra of polymer films were also recorded applying a Cary Eclipse spectrofluorimeter (Agilent Technologies, France), and the absorption spectra of these films were measured with an AVA-Spec-2048 spectrophotometer (Avantes, France), which allows one to record spectra in the range of 200–1100 nm.

3. Experimental results

Figure 2 shows the luminescence spectrum of OPBI films, which, in contrast to the spectrum of the initial solution (having a form of a wide band with a single maximum in the vicinity of 410 nm [18]), is a series of rather narrow bands near 430, 490, 510, 530, and 680 nm in the UV and visible spectral ranges.

The luminescence intensity from these films, excited by cw laser radiation with a wavelength of 405 nm and intensity of 6 W cm^{-2}, was found to rapidly decrease (by several times) for 2 or 3 s after the irradiation onset. It should be noted that, several seconds after the end of irradiation, the luminescence intensity was recovered to the initial level upon repeated excitation. Taking into account that the matrix has absorption above 10^3 cm^{-1} in this wavelength range (see Fig. 2 and data of [16]), this reversible effect of luminescence attenuation can be explained as a manifestation of the well-known mechanism of thermal quenching of luminescence [19] as a result of heating of the material under laser irradiation. As was noted in

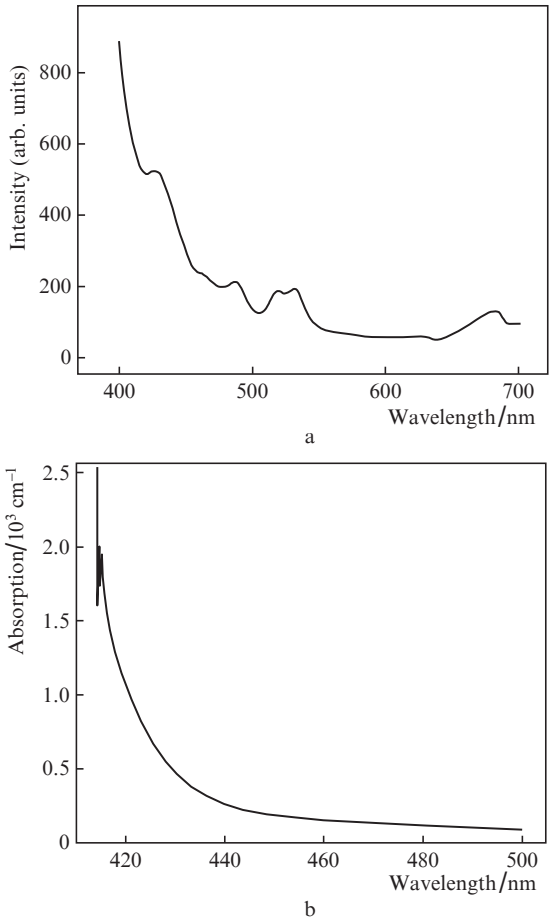

Figure 2. (a) Luminescence spectrum of a 10-μm-thick OPBI film (excitation wavelength 405 nm) and (b) its absorption spectrum.

[16], under cw laser irradiation at a wavelength of 532 nm and intensity of 15 W cm^{-2}, a film may be heated to 200 °C or higher. At even higher radiation intensities ($\sim 10^2$ W cm^{-2}) irreversible destructive effects were observed; they are related to the break of the polymer framework morphology in the film surface regions. These changes can be explained as follows: the aforementioned temperatures correspond to release of formic acid molecules, which are located in bound protonated states in benzimidazole chains and form a basis of the OPBI matrix [20, 21]. According to [22], these laser-induced processes in polymer matrices, accompanied by desorption of gas molecules in the polymer bulk, belong to swelling ones. An important process feature is the release of formic acid molecules and their condensation on certain matrix defects with the formation of bubble structures (the so-called swelling effect [22]) as a result of explosive boiling [17]. A further increase in the laser radiation intensity or dose may cause polymer carbonisation. At an incident radiation intensity of ~ 500 W cm^{-2} and minimum laser beam scanning velocities (5 mm s^{-1}), the fluence on the polymer film surface is ~ 1 J cm^{-2}.

Figure 3 shows photographs of the linear structures formed on the surface of an OPBI polymer film under laser irradiation (wavelength 405 nm, power 70 mW). When recording structures (Fig. 3a), the laser beam scanning velocity increased (starting with 5 mm s^{-1}) with a step of 5 mm s^{-1} when passing from strip to strip (from right to left). At the same time, the size of the laser beam spot on the film surface did not change. Photographs of fragments of selected strips in the luminescent light are shown in Fig. 3b. It can be seen that the laser-induced strip structures exhibit pronounced luminescence. The threshold laser power density, leading to the formation of luminescent structures, is ~ 1 kW cm^{-2}. The photographs obtained in both transmitted and luminescent light suggest that the width of each individual strip gradually decreases with an increase in the laser beam scanning velocity; the luminescence intensity decreases as well. If we suggest that the formation of bubble structures begins when exceeding a certain fluence threshold, the expansion of the formed strips with a decrease in the scanning velocity, which begins to be observed at some instant, is quite evident. Note also that luminescence of walls of individual bubble aggregates is observed well in these cases for the structures observed in luminescent light (the right bottom rectangle in Fig. 3b).

In another series of experiments, performed at a constant beam scanning velocity (10 mm s^{-1}), the focal length to the film surface was varied gradually: from strip to strip, with a step of 50 μm. The strip photographs, observed in transmitted light in an optical microscope, are presented in Fig. 3c. The extreme right strip corresponds to maximally exact focusing, whereas the extreme left strip corresponds to deviation from the focal plane by 2 mm. Segments of individual strips are shown on an enlarged scale in Fig. 3d. One can clearly see that, under exact focusing conditions, bubble structures are observed only over strip boundaries, whereas in the central part they are destroyed. In the defocusing regime (at successive removal by 1 mm from the focal plane), the entire strip consists of bubble structures.

The topographic images, recorded with a 3D optical microscope (Fig. 3e), show that the laser-induced structures rise above the film surface and consist of bubble clusters. The strip formed under exact focusing conditions (Fig. 3e, on the right) has a pronounced dip in the central part, which is obviously due to the destruction of bubble structures.

Figures 4a and 4b present SEM images of the structures obtained at low and high laser beam scanning velocities. A high beam scanning velocity allows one to obtain a thin laser strip, composed of integral bubble aggregates. At a low scanning velocity (Fig. 4a), wide strips are formed, with integral bubble aggregates on the periphery and fractured bubble structures in the central part.

The above results indicate the leading role of thermal processes in the formation of bubble structures in the surface regions of polymer film. Changing the laser radiation parameters, one can control the strip width. In other words, there is a range of laser fluences at which strips consist of only integral bubble structures.

AFM measurements yield useful information about the structure surface morphology. These measurements made it possible to determine the shape of individual bubble aggregates, which often turned out to be hemispherical (Fig. 4c). The results of modelling the distribution of photoluminescence intensity I_{PL} for such a thin-wall bubble on the film surface are shown in Fig. 4d. It was suggested that the thickness of the wall (luminescence source) is much smaller than the bubble size. It can be seen that the I_{PL} value is maximum at the periphery and rapidly decreases towards the bubble centre. Therefore, the 2D image of this bubble in luminescent light is a thin ring (Fig. 4d, inset). Such annular structures can clearly be observed in the laser strips formed on the OPBI film surface (Fig.3b). This fact confirms our suggestion about the

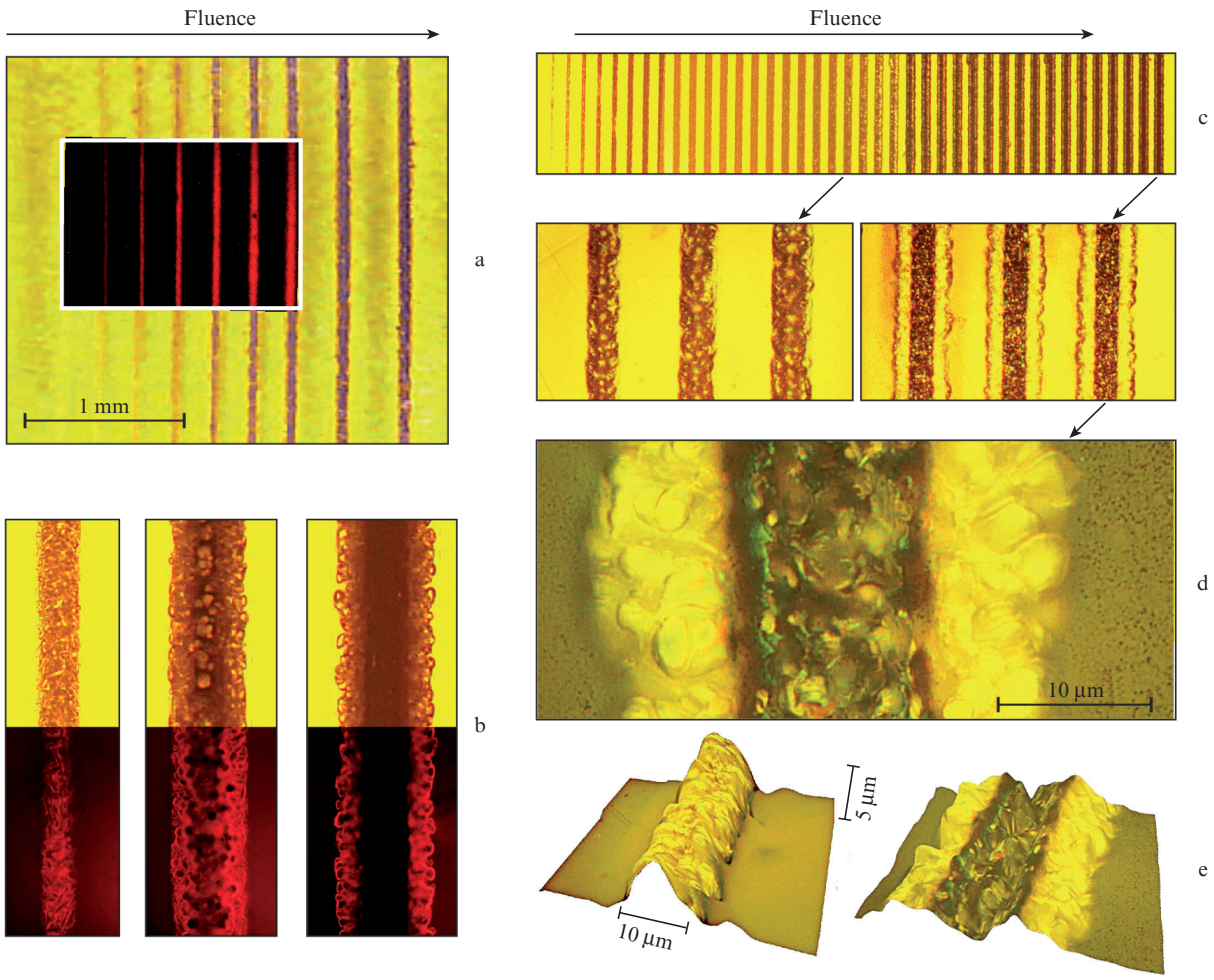

Figure 3. Photographs of an OPBI film with structures formed as strips: (a–d) measurements in (a) transmitted and (b) luminescent light with a change in the beam scanning velocity, (c) in transmitted light with a change in the focal length, and (d) in reflected light and (e) topographic images of fragments of individual strips, recorded on a 3D microscope.

decisive contribution of bubble structures to the luminescence signal.

AFM measurements also make it possible to trace the change in the sizes of an individual bubble aggregate in a strip (which does not contact other bubbles) during heat treatment. Successive annealing of a film sample to temperatures no higher than 150°C was found to lead to some decrease in the transverse sizes and increase in the height of individual bubbles (within 10%–15%), as demonstrated in Table 1. The error in measuring the bubble parameters did not exceed 5%. Films were not annealed to higher temperatures, because this annealing is accompanied by the formation of uncontrolled bubbles over the entire film surface (including the unirradiated areas) due to the activation of the release of residues of bound formic acid molecules from the matrix polymer and their subsequent condensation and boiling throughout the entire sample volume.

The results listed in Table 1 indicate a complex character of transformation of sizes and shapes of individual bubbles with an increase in the processing temperature, which may be related both to the desorption of formic acid molecules and to a change in the material plasticity upon heating. The latter may lead, in particular, to aggregation of small bubbles into larger ones (in the edge regions of individual structures), their break, or collapse. All these effects are most pronounced in the case of exact beam focusing (Fig. 4a).

Table 1. Dependences of the sizes of a laser-induced bubble on the OPBI surface and roughness of unirradiated area on the film annealing temperature according to the AFM data.

Annealing temperature (annealing time: 30–35 min)/°C	Bubble height (roughness)/nm	Bubble diameter/μm	Roughness of unirradiated area/nm
Before annealing	94 ± 5	10.0 ± 0.5	9.5 ± 0.2
80	105 ± 5	10.5 ± 0.5	7.9 ± 0.2
125	108 ± 5	10.3 ± 0.5	7.6 ± 0.2
150	107 ± 5	8.9 ± 0.5	5.5 ± 0.2

In view of the aforesaid, it is of interest to trace the change in the luminescence intensity from the structures during heat treatment. To this end, we studied the films subjected to laser irradiation in the defocusing regime, when the laser spot diameter on the film surface reached 100 μm. Specifically, we analysed the transverse luminescence intensity profile (averaged over strips) for individual linear structures, formed at different beam scanning velocities. The profiles obtained before and after several heat treatment cycles (heating a sample

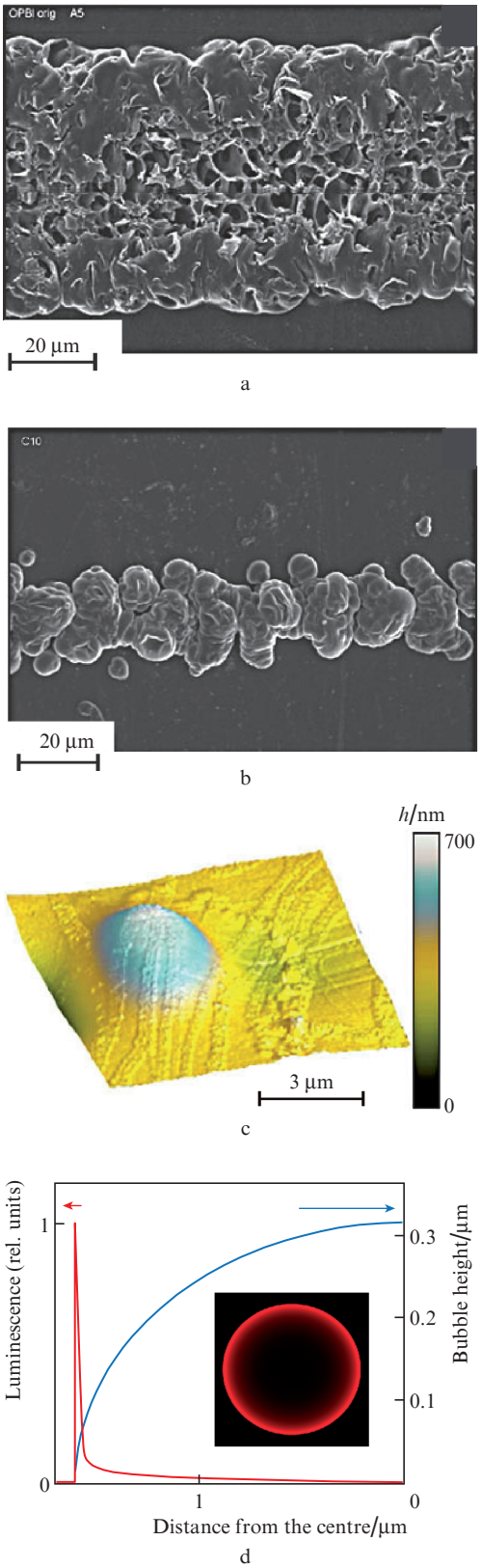

Figure 4. (a, b) SEM photographs of the bubble structures formed on the OPBI film surface at laser beam scanning velocities of (a) 5 and (b) 50 mm s^{-1}; (c) AFM image of an individual bubble in the structure formed on the film surface (c); and (d) results of simulating the luminescence intensity distribution I_{PL} for a thin-wall bubble on the film surface: dependences of the bubble height and I_{PL} on the distance to the bubble centre (the inset shows the 2D distribution of I_{PL}).

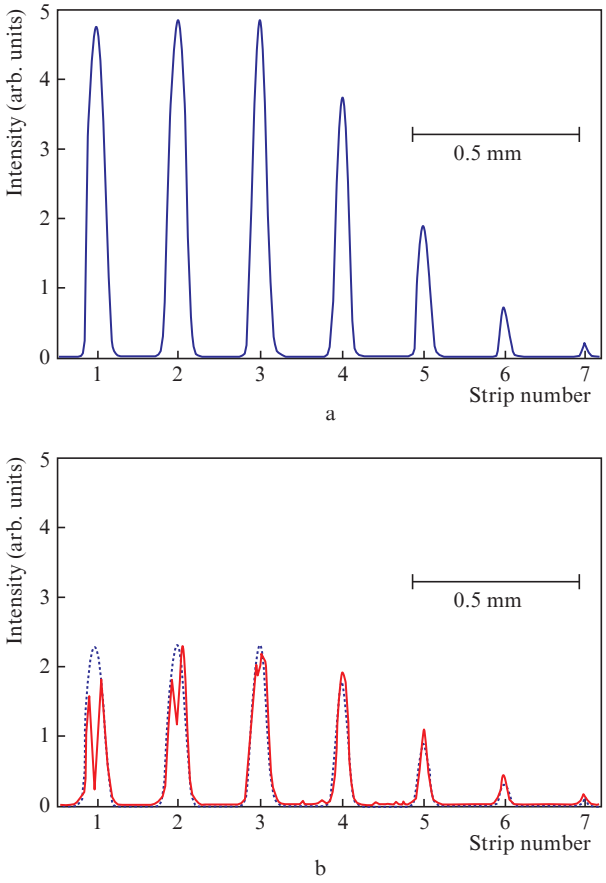

Figure 5. Averaged luminescence profiles for the observed structures, obtained by scanning a laser beam with velocities of (1) 5, (2) 10, (3) 15, (4) 20, (5) 25, (6) 30, and (7) 35 mm s^{-1}: (a) before the heat treatment and (b) after the second heating/cooling cycle (30 °C → 80 °C → 30 °C). The dotted curves are the profiles recorded before the heat treatment (with reduced amplitudes).

to 80 °C with its subsequent cooling to 30 °C) were compared. The results showed that, even after the first or second heating cycle, the luminescence intensity irreversibly dropped for all observed structures (Fig. 5). Nevertheless, it remained higher than the luminescence from the unirradiated film surface (in the gaps between the laser-induced structures). Note the occurrence of clearly observed dips in the luminescence intensity curves for the first three heat-treated structures (Fig. 5b, solid lines). Geometrically, these dips correspond to the axial lines of individual luminescent structures.

It can be seen in Fig. 5b that the depth of the dip induced by the heat treatment in the averaged luminescence signal profile decreases with an increase in the structure formation rate. A comparison of the luminescence intensity profiles for individual structures before and after heat treatment shows that their widths practically coincide (despite the presence of dips). This fact indicates that, after carrying out the second heating/cooling cycle (30 °C → 80 °C → 30 °C), a certain number of luminescent elements (bubbles) are 'burnt out' in the central region of strips 1–3 (Fig. 5b). This can be explained by considering again the images of the structures obtained in different beam focusing regimes (different fluences on the film surface) by 3D microscopy (Fig. 3b) and SEM (Fig. 4). It can be seen that bubbles collapse along the axial line of newly

formed strips at large fluences. This process leads to disappearance of the polymer regions with 'stretched' polymer chains in the central part and, therefore, disappearance of new luminescence sources. The same situation occurs in the case of additional film heating on the heating element (Fig. 5b), when pronounced dips arise in the central regions of luminescence profiles. One of possible reasons for the absence of a systematic decrease in the luminescence intensity within the three first strips (Fig. 5a) with an increase in the formation rate is the influence of the film surface carbonisation, which occurs at large laser irradiation doses (see Fig. 3d). In principle, the same effect may contribute to some extent to the depth of dips in the observed luminescence profiles for these structures.

Similar situations with the increase in the luminescence intensity in stretched polymer matrix regions (to which bubble aggregates belong, in our opinion) are also implemented under mechanical impacts on a film. For example, this situation occurs during bending or cut-like deformation of an OPBI film (Fig. 6). It can be seen that the bending and cut regions are observed as brighter luminescent structures against the background of the rest of the film. Thus, a polymer matrix can be considered as a medium whose luminescence properties depend on external (laser, mechanical) impacts and which may retain for a long time a stable luminescence response induced by these impacts.

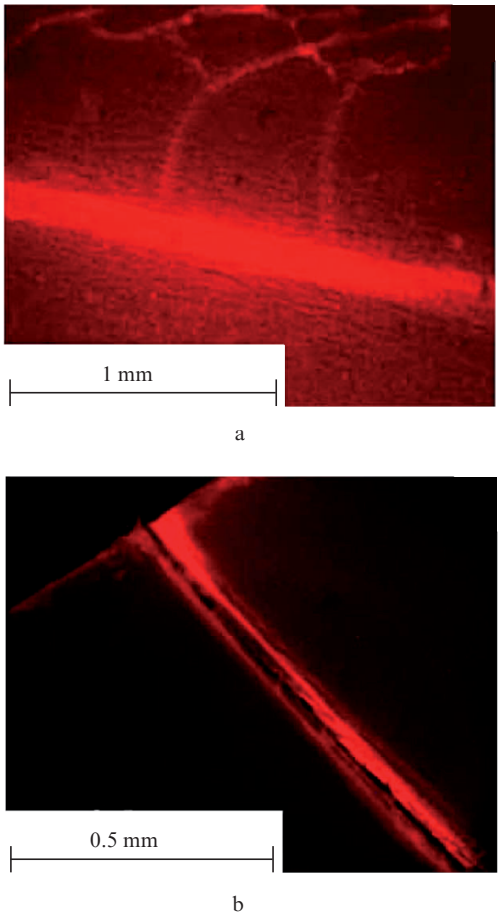

Figure 6. Photographs of the luminescent structures obtained under different mechanical impacts on an OPBI film: (a) bending deformation and (b) through cut.

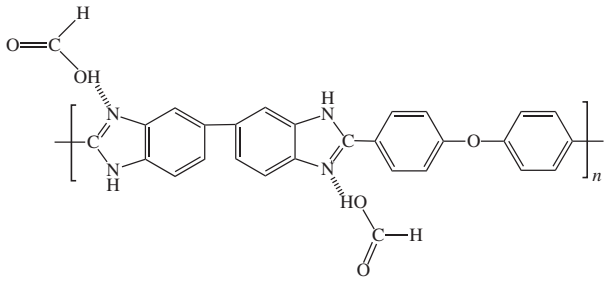

Figure 7. Structural fragment of benzimidazole with associated formic acid molecules in the protonated state.

4. Results and discussion

All the aforementioned phenomena, related to changes in the luminescence properties of polymer film regions subjected to laser irradiation or mechanical impact, can be explained taking into account the effects of concentration quenching of luminescence centres existing in such polymer matrices. Indeed, as was noted in [18], excitation of a polybenzimidazole solution in formic acid by 380-nm radiation induces green luminescence in the solution. According to the data of [18, 20, 21], the solution luminescence band has two maxima in the vicinity of 405 and 460 nm, which are due to the transition from the excited ^1L_b level to two lower vibrational states. This system of levels belongs to the imidazole ring (containing nitrogen atoms), which is, in turn, conjugate with the benzene ring in polybenzimidazole molecules (Fig. 7). The intensity of this band decreases with an increase in the molecular concentration in such solutions, but, at the same time, a wide band peaking at 550 nm arises. The decrease in the first-band intensity is a manifestation of the effects of luminescence concentration quenching [19], while the occurrence of the long-wavelength band is explained by the formation of more complex aggregated complexes in polybenzimidazole chains [18]. As follows from the data presented in Fig. 2, luminescence bands of similar nature are most likely implemented in solid OPBI films as well, although with pronounced distinctions; the results of a more detailed study of the spectroscopic properties of these films will be reported separately.

According to our measurements (Fig. 2), a solid OPBI film also exhibits a group of weak luminescence lines of the same nature in this region. We may suggest that the luminescence centres related to the structural elements of polymer matrix are more closely spaced (at distances of few nanometres) in solid films as compared with the initial solutions, which results in efficient luminescence quenching [23, 24]. In these situations, when the distance between luminescence centres of the same type does not exceed few nanometres, the excitation energy transfer from one donor centre D to another is known to occur according to the dipole–dipole resonance mechanism [23]. The probability of this process is $k \propto r^{-6}$, where r is the distance between the nearest D centres. In this case, the excitation energy transfer and relaxation occur according to the following scheme: D → D …→ A, where A are nonradiatively absorbing centres, e.g., molecules of water, oxygen, and some other impurities [24]. For the centres with characteristic times of radiative luminescence decay of $\sim 10^{-9}$ s (to which luminescent centres in the OPBI matrix belong [20]), efficient excitation energy transfer occurs when the dis-

tance between them does not exceed 4–10 nm [23]. In our situation the distance between the nearest luminescence centres in benzimidazole rings is on the order of 1 nm. Hence, it is obvious that even small increments in r may reduce significantly the k value and, correspondingly, increase the probability of radiative relaxation of the D centre. Note that the luminescence intensity may rise with an increase in the specific surface area. The reason is that the luminescence efficiency of the centres located on the surface is higher because of the less dense environment [25].

The aforementioned changes may occur during laser-induced formation of strips. Indeed, due to the extension, the distance between luminescence centres in bubble foam-like structures formed on the OPBI film surface (Fig. 3) is larger than in the unirradiated region. In addition, foam-like structures have a large specific surface area. Therefore, because of the decrease in efficient luminescence quenching according to two mechanisms, the luminescence intensity in bubble structures significantly increases.

Similar situations, related to the increase in the distances between luminescence centres and growth of the specific surface area, should also be implemented under mechanical impacts on a film, for example, in the region of its bending without mechanical damage (Fig. 6a) or cut (Fig. 6b). On the whole, such a system with closely spaced luminescence centres in a matrix can be considered as a nano- and microstructured (with respect to these centres) medium, which is fairly sensitive to any external effects. Thermal (including laser) (Fig. 3) or mechanical (Fig. 6) impacts cause a local increase in the specific surface area and occurrence of stretched regions, thus forming a long-term impression that can easily be observed in luminescent light.

Currently, there is much interest all over the world in searching and designing new foam-like matrices, which can be applied in various fields of science and technology: from biotechnologies to synthesis of various catalytic systems (see, for example, [26–30]). The use of the effects demonstrated above on an example of OPBI film opens ways for forming new functional devices by further miniaturisation of bubble structures using femtosecond laser radiation.

5. Conclusions

We reported for the first time experimental results demonstrating the possibility of forming luminescent structures on the surface of heat-resistant OPBI films synthesised by the coating method from a formic acid solution. The structures were obtained using a focused cw 405-nm laser beam. It was shown (using optical, atomic-force, and scanning electron microscopy) that these luminescent structures consist of bubble micrometer-sized aggregates, located on the film surface. A bubble formation model was proposed, which implies manifestation of the swelling effect during intense release of formic acid molecules from protonated states in the polymer matrix, their condensation, and explosive boiling as a result of intense heating by laser radiation. The enhancement of the luminescence from bubble aggregates is related to the attenuation of concentration quenching for the luminescence centres (ring fragments in imidazole chains) during their emergence on the surface and increase in the distance between them in stretched (bubble) matrix regions.

Acknowledgements. The authors wish to dedicate this paper in the memory of V.N. Bagratashvili.

We are grateful to O.I. Gromov (Faculty of Chemistry, Moscow State University) for the helpful consultations.

This work was supported by the Russian Foundation for Basic Research (Grant No. 18-29-06056 in the part concerning the laser structuring of materials and Grant No. 18-33-00645 in the part concerning the synthesis of polymer OPBI films) and by the Ministry of Science and Higher Education of the Russian Federation within the State assignment for the Federal Scientific Research Centre 'Crystallography and Photonics' of the Russian Academy of Sciences in the part concerning the development of laser methods for forming microstructures.

References

1. Shimotsuma Y., Kazansky P.G., Qiu J.R., Hirao K. *Phys. Rev. Lett.*, **91** (24), 242405 (2003).
2. Liang F., Vallee R., Chin S.L. *Opt. Express*, **20**, 4389 (2012).
3. Davis K.M., Miura K., Sugitomo N., Hirao K. *Opt. Lett.*, **21** (21), 1729 (1996).
4. Marla D., Andersen S.A., Zhang Y., Hattel J.H., Spandenberg J. *J. Manuf. Processes*, **32**, 432 (2018).
5. Qu S., Zeng H., Zhao C., Qiu J., Zhu C. *Chem. Phys. Lett.*, **384**, 382 (2004).
6. Bagratashvili V.N., Rybaltovskii A.A., Rybaltovskii A.O., Minaev N.V., Tsypina S.I., Panchenko V.Ya., Zavorotnyi Yu.S. *Laser Phys.*, **20**, 139 (2010).
7. Bagratashvili V.N., Minaev N.V., Rybaltovskii A.O., Yusupov V.I. *Laser Phys. Lett.*, **8** (12), 853 (2014).
8. Askins C.G., in *Defect in SiO_2 and Related Dielectrics: Science and Technology.* Ed. by G. Pacchioni, L. Skuja, D.L. Griscom (Dordrecht: Springer, 2000, NATO Science Series, Ser.II: Mathematical and Phys. Chem.) Vol. 2, pp 391–426.
9. Baraban A.P., Dmitriev V.A., Gadzhala A.A. *Russ. Phys. J.*, **57** (5), 627 (2014) [*Izv. Vyssh. Uchebn. Zaved., Ser. Fiz.*, **57** (5), 56 (2014)].
10. Dirr S., Wiese S., Johannes H.-H. *Synth. Mater.*, **91** (1-3), 53 (1999).
11. Kydrius T., Slekys G., Juodkaziz S. *J. Phys. D: Appl. Phys.*, **43**, 145501 (2010).
12. Sun H.-T., Sakka Y. *Sci. Technol. Adv. Mater.*, **15** (1), 014205 (2014).
13. Lin C.-A.J., Lee C.-H., Hsieh J.-T., Wang H.-H., Li J.K., Shen J.-L., Chan W.-H., Yeh H.-I., Chang W.H. *J. Med. Biolog. Eng.*, **29**, 276 (2009).
14. Kunwar P., Hassinen J., Bautista G., Ras R.H.A., Toivonen J. *ACS Nano*, **8**, 11165 (2014).
15. Li J., Zhu J.-J., Hu K. *Trends Anal. Chem.*, **58**, 90 (2014).
16. Akovantseva A.A., Aksenova N.A., Zarkhina T.S., Krotova L.I., Minaev N.V., Rybaltovskii A.O., Kholkhoev B.Ch., Farion I.A., Yusupov V.I., Burdukovskii V.F., Bagratashvili V.N., Timashev P.S. *Zh. Prikl. Khim.*, **90** (1), 91 (2017).
17. Zhigar'kov V.S., Yusupov V.I., Tsypina S.I., Bagratashvili V.N. *Quantum Electron.*, **47** (10), 942 (2017) [*Kvantovaya Elektron.*, **47** (10), 942 (2017)].
18. Ghosh S., Sannigrahi A., Maity S., Jana T. *J. Phys. Chem. B*, **114**, 3122 (2010).
19. Lakovicz J.R. *Principles of Fluorescence Spectroscopy* (Springer, 2006) p. 954.
20. Kojima T. *J. Polym. Sci. Part B: Polym. Phys.*, **18**, 1685 (1980).
21. Sannigrahi A., Arunbabu D., Sankar R.M., Jana T. *Macromolecules*, **40**, 2844 (2007).
22. Bityurin N.M. *Quantum Electron.*, **40** (11), 955 (2010) [*Kvantovaya Elektron.*, **40** (11), 955 (2010)].
23. Agranovich V.M., Galanin M.D. *Electronic Excitation Energy Transfer in Condensed Matter* (Amsterdam: North Holland, 1983; Moscow: Nauka, 1978).

24. Leonenko I.I., Aleksandrova D.I., Egorova A.V., Antonovich V.P. *Metody Ob'ekty Khim. Anal.*, **7** (3), 108 (2012).
25. Yusupov V.I., Bagratashvili V.N. *Langmuir.*, **34** (43), 12794 (2018), DOI:10.1021/acs.langmuir.8b01721.
26. Gaspard S., Oujja M., Abrsci C., Catalina F., Lazare S., Desvergne J.P., Castillejo M. *J. Photochem. Photobiol. A*, **193**, 187 (2008).
27. Castillejo M., Rebollar E., Oujja M., Sauz M., Selimis A., Sigletou M., Psycharakis S., Ranella A., Fotakis C. *Appl. Surf. Sci.*, **258**, 8919 (2012).
28. Leonova E.V., Gotovtseva E.Yu., Izaak T.I., Svetlichnyi V.A., Biryukov A.A. *Izv. Vyssh. Uchebn. Zaved., Ser. Fiz.*, **9** (2), 58 (2011).
29. Sasikala S.P., Poulin P., Aymonier C. *Adv. Mater.*, **28**, 2663 (2016).
30. Rybaltovskii A.O., Arakcheev V.G., Bekin A.N., Danilyuk A.F., Gerasimova V.I., Minaev N.V., Golubeva E.N., Parenago O.O., Bagratashvili V.N. *Sverkhkrit. Flyuidy: Teor. Prakt.*, **9** (4), 61 (2014).